IEEE Access
Multidisciplinary ⋮ Rapid Review ⋮ Open Access Journal

Received 27 January 2024, accepted 11 February 2024, date of publication 20 February 2024, date of current version 28 February 2024.

Digital Object Identifier 10.1109/ACCESS.2024.3368038

RESEARCH ARTICLE

A Planning Model for an Electric Vehicle Aggregator Providing Ancillary Services to an Unbalanced Distribution Network Considering Contract Design

AMMAR M. MUQBEL[1], (Student Member, IEEE), ALI T. AL-AWAMI[1,2], (Senior Member, IEEE), AND ADNAN S. AL-BUKHAYTAN[1], (Student Member, IEEE)

[1]Department of Electrical Engineering, King Fahd University of Petroleum and Minerals (KFUPM), Dhahran 31261, Saudi Arabia
[2]Interdisciplinary Research Center for Smart Mobility and Logistics, King Fahd University of Petroleum and Minerals (KFUPM), Dhahran 31261, Saudi Arabia

Corresponding author: Ammar M. Muqbel (ammar.muqbel@kfupm.edu.sa)

This work was supported by King Fahd University of Petroleum and Minerals and King Abdulaziz City for Science and Technology (KACST) under Project 14-ENE360-04.

ABSTRACT Recent advancements in battery technology have made them more economically viable than ever before, making them suitable for various grid-scale applications. Due to their rapid response, batteries are attractive for providing ancillary services (AS), such as frequency regulation and reserve services, to the bulk power grid. On the other hand, an electric vehicle (EV) is viewed as a moving battery; consequently, EVs are also suitable for those services. This research proposes a linear planning model for an Electric Vehicle Aggregator (EVA) within a distribution network (DN) to offer Ancillary Services (AS) to the bulk power grid. The model takes into account contract design by identifying optimal incentives or charging tariffs that Electric Vehicle (EV) owners would be willing to pay the EVA for charging their vehicles. Additionally, the model takes into account the size of the electric vehicle (EV) fleet as a crucial planning factor for EV aggregation that depends on the energy pricing set by the EVA. The proposed model is developed to maximize the overall profit of bidding capacities in the energy and AS markets while supporting the operation of an unbalanced DN by maintaining the DN limits. Simulation results and sensitivity analyses on the model have been carried out to support the investment model and investigate the change in the optimal solution across different case studies. Simulations show that the optimal charging tariff (β) is (0.02 $\$/kWh$)when considering scenarios where Distribution Network (DN) limits, such as thermal and voltage constraints, are ignored for all EV participation versus β relations. When including the DN, the optimal payoffs vary based on the relationship between the charging tariff and the number of participating EVs.

INDEX TERMS EV aggregators,V2G, G2V, planning model, unbalanced distribution network, ancillary services, electricity market.

NOMENCLATURE

INDICES

A, B, C	Index of phases.
e	Index of EV.
k	Index of bus.
t	Index of hour.
d	Index of day.
w	Index of week.
y	Index of year.

PARAMETERS AND CONSTANTS

B^{AB}	The admittance matrix imaginary part that links between phase A and phase B.
$BatC$	Cost of battery replacement($\$/kW$).
BiC	Cost of retrofitting for bidirectional V2G ($\$/kW$).

The associate editor coordinating the review of this manuscript and approving it for publication was Jahangir Hossain.

ChC	Cost of charger ($\$/kW$).
$ComC$	EV's communications cost ($).
E	Energy needed for scheduled trip at $t = \tau^p(kWh)$.
G^{AB}	The admittance matrix real part that links between phase A and phase B.
$J^{AB}_{P\theta}$	A matrix that links real power from phase A with voltage angle from phase B.
J^{AB}_{QV}	A matrix that links reactive power from phase A ith voltage magnitude from phase B.
NY, NW	Years and weeks number.
NT	The number of available EVs in the area.
NEV	Number of EV usage profiles.
NP	Total number of scheduled trips per day.
r	Discount rate.
SC	EV's smart meter cost ($).
T	Total hours in a day (hours).
$\alpha^{D,U.R}$	Estimated regulation down, regulation up, and responsive reserve commands (as % of bid capacities).
$\sigma^{D,U,R}$	regulation down, regulation up and responsive reserve forecasted prices ($\$/kWh$).
σ^E	Forecasted energy price ($\$/kWh$).
π	The departure probability of a random EV.
π^A	Accumulated departure probability of EV.
ω_t	The expected available EVs percentage to perform V2G at time t.
δ	Compensation factor for unplanned departures.
η	efficiency of charging and discharging.
φ, ϕ	The permissible Minimum and maximum SOC limits (as % of the energy capacity (MC)).
τ^P	Trip time for p-th scheduled trip.
ν	EV availability; 1 if EV is available, 0 otherwise.

DECISION AND AUXILIARY VARIABLES

AD^D, AP^U AP^R	Power capacity available for regulation down, regulation up, and reserves (kW).
DC	Discharging cost ($\$/kWh$).
$E\|\cdot\|$	Expected value.
FP^-	Conservative estimation of final power draw.
g	EV depreciation cost paid by EVA to EV owners.
$InvC$	Investment cost ($).
MP, MC	Maximum power (kW) and energy ratings (kWh).
OpP	Annual operation profits ($).
OpI, OpC	Expected daily operational income and cost to EVA.
P^A_{kj}	Power transferred in phase A between k and j.
P^A_k, Q^A_k	The injected real and reactive power vectors in phase A and bus k.
POP	Preferred operating point (kW).
$R^{D,U,R}$	EVA's capacity bid of regulation down, regulation up and responsive reserve (kW).
SOC	Estimated energy in the battery (kWh).
TP	Project's total payoff ($).
V^A_k, θ^A_k	Voltage magnitude and angle for bus K.
β	Energy tariff paid by the EV's owners ($\$/kWh$).
γ	EV aggregation percentage of participation.

I. INTRODUCTION

A. MOTIVATION AND BACKGROUND

The transportation sector is a major consumer of energy from fossil fuels, as evidenced in the US, where it accounts for approximately 27% of total energy consumption [1], and in Saudi Arabia, where it constitutes around 26.87% [2]. Hence, replacing conventional vehicles that consume fossil fuels with electric vehicles (EVs) contributes to reducing greenhouse gas emissions dramatically. Although EVs positively impact the environment by reducing greenhouse gas emissions, the rapid increase in the number of EVs used can boost energy demand on the grid. Moreover, this may introduce new challenges to the grid and necessitate increasing fossil fuel generators' capacity.

With the depletion of natural resources and increasing global warming, distributed renewable energy resources (RESs) such as wind turbines (WT) and photovoltaic (PV) are preferred over fossil fuel generators to minimize greenhouse gas emissions. However, high penetration of RESs will introduce safety and technical challenges to the grid since RESs are stochastic and weather-dependent [3]. One effective solution to address the challenges caused by RESs is to install a stationary battery energy storage system (BESS), which can be charged or discharged to balance out any surplus or deficit in the energy generated by RESs. This approach helps ensure a stable and reliable energy supply, while simultaneously reducing the environmental impact of energy production [4]. Despite the decreasing cost of stationary BESS, it is still too expensive for most grid-tied applications [5]. EV batteries can be used for vehicle-to-grid (V2G) services, where they extract or inject power into the grid while parked, similar to BESS.

V2G represents the system that facilitates the exchange of ancillary services (AS) through bidirectional energy flow between the grid and plugged-in EVs [6]. Two methods of V2G operations are presented in [7]. The first method is unidirectional V2G, which considers EVs as controlled loads to provide AS to the grid and to charge them during off-peak hours to reduce peak-hour stress. The second method is the bidirectional V2G, which allows EVs to both charge and discharge their batteries to support the grid.

Although EV owners may obtain some benefit by providing services to the grid individually, the use of EVs for V2G regulation becomes practical only when a considerable number of EVs are managed jointly, and the resulting services are controlled by an EV aggregator (EVA) [8]. The EVA acts as an intermediary between EV owners and the independent system operator (ISO), organizing distributed small-scale

generation and storage resources to offer large-scale services to the grid, such as regulation and capacity bidding.

EVA submits bids for energy to the day-ahead (DA) energy market to purchase energy at market prices and then sells this energy to EV owners at a fixed tariff. The EVA is also able to participate in the AS market by providing regulation up/down and reserve capacity through the charging/discharging of EVs. If the AS market accepts the bids for either regulation up/down, the EVA will adjust the charging/discharging of EVs accordingly, based on market signals. However, EVA is expected to compensate EV owners for these services.

The main objective of the EVA is to maximize its overall profits while ensuring the satisfaction of EV owners and maintaining distribution network (DN) limits at acceptable levels. This study aims to optimize the EVA's profitability through strategic bidding capacity and participation in the AS markets, providing regulation up/down and reserves for the grid. The number of EVs participating in the AS market will be a decision variable used to determine the most advantageous incentives or charging tariffs that EV owners will pay the EVA for charging their EVs.

B. LITERATURE REVIEW

Control strategies are necessary for managing the charging/discharging powers of EVs to provide AS. Current V2G regulatory strategies include the grid measurement approach [9] and the optimization-based approach [10]. Both assumed that EVs follow schedules set by the ISO or EVA for grid optimization. However, these approaches may not be practical for real-world operations since EVs are owned by various individuals that present challenges for the ISO to manage signals collectively. Furthermore, these methods may inconvenience EV owners, who would lack control over the timing and amount of their bids. Several studies have explored the most effective operational bidding strategies for EVAs in energy markets. EV batteries, with their rapid response capabilities, have the potential to significantly support the bulk power grid by providing AS [11]. According to [12] and [13], EVs can also contribute to primary frequency regulation in both large-scale systems and microgrids.

The authors of [14] investigated the concept of EV participation in AS using a robust optimization framework. In [15], the objective of the EVA was to minimize the total charging cost by shifting EV charging to times of lower prices, while also maximizing revenue from participating in AS. Additionally, this strategy can provide AS and offer flexibility to help alleviate congestion during peak hours. However, the studies presented in [11], [13], [14], and [15] assumed that the operation was limited to unidirectional power flow from the grid to the EVs.

EV owners can offer frequency regulation capacities to the power grid, as suggested in [16]. The EVA submits the available regulation capacity to the market at each time step, taking into account the convenience of EV owners. However, it does not account for the optimal scheduling of charging/discharging to alleviate congested loads. Reference [17] explored a detailed model of interactions between competing EVs and the EVA, with the EVA determining the energy trading price and the EVs formulating their charging/discharging strategies. Additionally, the EVA collaborates with EVs to enhance their collective social welfare. The limitation of this model is that it considers regulation up and down but overlooks reserve capacity. In [18], an aggregator is described that gathers power usage plans from home management systems for AS market participation, considering energy consumption, vehicle usage, and generation. Stochastic optimization is used in [15] to integrate EVs into the regulation market and analyze the economic benefits of bidding in the DA energy market. However, the studies in [15] and [18] did not address the impact of battery degradation on associated EVs. It should be noted that references [15], [16], [17], and [18] focus solely on operational models rather than strategic planning.

In [19], [20], and [21], a comprehensive optimization model for V2G was studied. In [19], the EVA optimized EV operations for AS market participation, taking into account a fleet of 10,000 EVs. Reference [20] provided a comparison of unidirectional and bidirectional V2G approaches for offering frequency regulation and reserve services. The aggregators' role, as described in [19] and [20], involved coordinating with the ISO to purchase energy for charging EVs and to place bids in the AS market. In [21], the study was extended to include bidirectional V2G while factoring in the cost of battery degradation. Additionally, a dispatch algorithm was developed to minimize daily operational costs within a centralized system comprising EVs, BESS, and RESs.

The inclusion of degradation costs in the EVA model for V2G operational bidding strategies was addressed in [22], [23], and [24]. The authors of [22] developed a mixed-integer linear programming approach for aggregated EVs in the AS market to minimize frequency deviation and enhance revenue. The research presented in [23] introduced a strategy for the EVA to perform energy arbitrage by aggregating EVs and providing charging services, aiming to maximize future market profits while considering uncertainties in EV departure times and movement. In [24], the feasibility of EVA participation in energy and AS markets for profit maximization was investigated using the Generalized Reduced Gradient method to address the non-linear programming challenges, with the New York competitive market as a case study. However, these studies primarily explored operational considerations without addressing the strategic planning aspect for EVA.

In terms of planning, much of the EV-related research, such as in [25], [26], and [27], focuses on charging stations. The authors of [25] introduced a multi-objective evolutionary algorithm to strategically locate charging stations within a radial DN for a specified number of EVs. In [26], a second-order conic optimization model was developed to minimize power losses by considering RESs (PV and WT), BESS, and EV charging stations. The authors of [28] aimed to optimize the installation of RESs and EV demand for each aggregator,

with an emphasis on loss reduction, while implementing generation curtailment and EV controllability to maintain the DN constraints. However, these studies did not incorporate cost impacts into their objective functions. The authors of [27] addressed the life cycle of BESS when integrated with charging stations. The studies [25], [26], [27], and [28] utilized nonlinear models that pose challenges in large-scale power systems, and they assumed a fixed number of EVs without considering dynamic sizing or incentive tariffs for EV owners. The research in [29] and [30] explored a centralized BESS's bidding approach in coordination with EVs for AS market participation. They focused on optimal BESS sizing to regulate EV participation error within acceptable market limits and aimed to minimize response discrepancies. Nonetheless, they did not account for the degradation costs of EV batteries or the BESS, nor did they factor in the DN in their models.

C. CONTRIBUTIONS

Based on the extensive literature review, it is evident that most studies have focused on the optimal operation of EVs by scheduling the charging and discharging to maximize profits. Additionally, research has concentrated on siting charging stations within nonlinear DN models, which presents challenges for large-scale planning. Consequently, there is a need for a comprehensive and scalable EVA planning model tailored to AS provision in market environments. To address this, the paper proposes a detailed planning model for the EVA, characterized by the following attributes:

- A linear planning EVA model is proposed for AS market participation and grid service provision. This model determines the optimal fleet size of EVs that balances the potential income against the associated investment costs. It does so by optimizing the number of EVs to ensure maximum profitability for the EVA, considering the trade-off between higher revenue with larger fleets and the investment costs for infrastructure (SC), communication ($ComC$), and bidirectional chargers (BiC).
- The proposed model evaluates the investment feasibility of establishing an EVA within an unbalanced DN, focusing on contract design by determining the most attractive incentives or charging tariffs that EV owners will pay the EVA for the service of charging their EVs.
- To ensure scalability, the proposed EVA planning model is formulated as a fully linear model and incorporates linearized constraints for the DN, such as voltage levels and line capacity limits. It is important to note that none of the existing EV planning models in the literature, such as those reported in [25], [26], [27], and [29], have taken into account these linearized DN constraints.
- The proposed model accounts for technical and market constraints. Furthermore, it identifies the optimal operational decisions for EVs, including bidding capacities and operating points, using the model.

D. PAPER ORGANIZATION

The rest of the paper is organized as follows: the details of the proposed planning model for EVA planning aggregation and DN planning model are provided in Section II-A and Section II-B, respectively. The optimization model and methodology for EV planning are discussed in Section III. The case study that assesses the proposed model in the energy market is provided in Section IV, whereas the obtained results are provided in Section V. Finally, a few concluding remarks are given in Section VI.

II. PROPOSED PLANNING MODEL FOR EV AGGREGATION

This section demonstrates how the EVA optimizes its participation in the AS market by bidding for regulation up/down and reserving capacity. The EVA planning model is detailed in Section II-A. Subsequently, the linear EVA model will be integrated with the unbalanced DN linear model (presented in Section II-B) to examine the impact of DN constraints on the optimal results

A. EV AGGREGATOR (EVA) PLANNING MODEL

In this work, the EVA consolidates individual EVs to participate in the AS market. The EVA buys the energy from the Day-Ahead (DA) energy market at the market price (σ^{E}_{tdw}) to provide charging services to EVs' owners at a fixed tariff (β). In the AS market, the EVA offers bids for regulation up (AP^{U}_{tdw}), regulation down (AP^{D}_{tdw}), and reserve services (AP^{R}_{tdw}). These services are priced according to the regulation up price (σ^{U}), regulation down price (σ^{D}), and reserve capacity price (σ^{R}), as illustrated in Figure 1. Regulation up and down services involve real-time, different from reserves, and adjust the charging rates to align with real-time grid requirements, maintaining the balance between

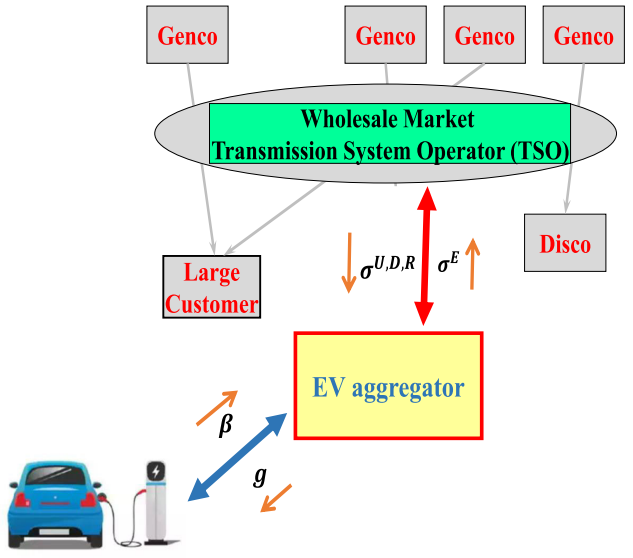

FIGURE 1. EV aggregator planning model in a pool-based electricity market for energy and AS.

supply and demand. Reserves, on the other hand, stand as a contingency against unexpected grid events. It should be noted that the hourly market price for each service varies. Most markets, including the Electric Reliability Council of Texas (ERCOT) [31] and the California Independent System Operator (CAISO) [32], distinguish between regulation services, such as regulation up and regulation down, and reserve capacity. This differentiation is attributed to their different operational characteristics and requirements.

The EVA requests EVs' owners to provide AS by adjusting the charging rate around a preferred operating point (POP). The POP's adaptability for each service type is depicted in Figure 2, illustrating the dynamic nature of the model in optimizing these services. To clarify the concept of the POP, consider that the EVA bids a regulation up capacity for a particular hour t. In this scenario, the POP is adjusted downward in response to the AS market signal, with the maximum allowable adjustment corresponding to the bid capacity. It means that the EV's owner reduces its charging rate, which means providing regulation up to the network. Conversely, in the scenario of regulation down, the EVA requests the EV owners to increase the charging rate, which increases the load consumption and thus provides regulation down to the network. For reserve capacity and real-time operations, the EV owners have agreed to reduce their load consumption in the event of a contingency and upon request from the EVA.

It is important to note that extracting energy from EVs can reduce their battery lifespan. Consequently, the EVA compensates EV owners at a constant rate, which is determined based on the battery costs during the period under study [33].

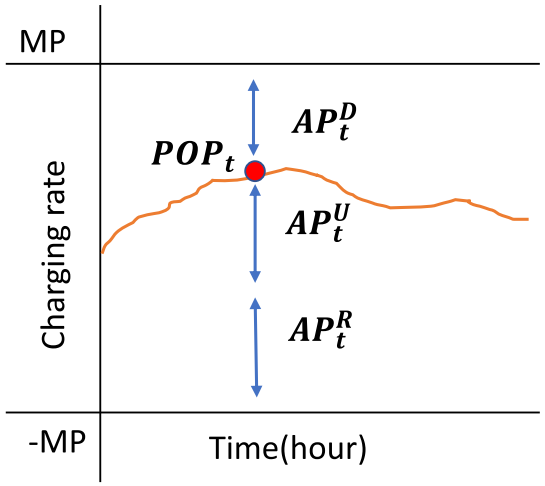

FIGURE 2. Regulation up/down and reserve capacities around the charger operating point (POP).

It shall be noted that each participating EV has a travel profile that includes many pre-planned trips. It is anticipated that unexpected departures may occur randomly throughout the day, making the EV unavailable for V2G during certain periods. This variability is managed by calculating the percentage (ω_t) of the EV's remaining capacity available for V2G. The variable v_{it}, which is binary, is used to denote whether an EV is available at a particular time of day.

B. DISTRIBUTION NETWORK MODEL

The planning problem is considered a challenging task, requiring an extensive amount of time to solve. Utilizing a full Alternating Current (AC) power flow model would render the problem nearly insurmountable, thereby necessitating the use of a linear model for the DN. The proposed model in [34] is employed to linearize the unbalanced DN model and to conduct a three-phase load flow analysis. This linear model is utilized because it offers a compact framework suitable for an unbalanced DN and integrates easily with the linear model of the EVA. Furthermore, it provides voltage magnitudes and phase angles with high accuracy, as validated in this work. This model is underpinned by the following two equations:

$$P_k^A = V_k^A \sum_{j}^{N} \sum_{B}^{A-C} V_j^B (G_{kj}^{AB} Cos(\theta_{kj}^{AB} + B_{kj}^{AB} Sin\theta_{kj}^{AB}) \quad (1)$$

$$Q_k^A = V_k^A \sum_{j}^{N} \sum_{B}^{A-C} V_j^B (G_{kj}^{AB} Sin(\theta_{kj}^{AB} - B_{kj}^{AB} Cos\theta_{kj}^{AB}) \quad (2)$$

The two equations in (1) and (2) represent the injected real and reactive power at bus k, respectively. It is clear that both equations are nonlinear, and to linearize them, the following assumptions are made:

1) The voltage angle between two nodes is sufficiently small due to the short distance. As a result, the value of θ_{kj}^A shall be close to zero, so $Sin\theta_{kj}^A$ and $Cos\theta_{kj}^A$ can be approximated to zero and one, respectively.
2) In normal conditions, the voltage magnitudes are close to one, and any change in voltages will be around one. Hence, it can be assumed that $V_k = (1 + \Delta V_k)$ and $V_j = (1 + \Delta V_j)$ where ΔV_k and ΔV_j are the change in the voltage from the nominal value.

Hence the multiplication of two voltages is linearized as follows:

$$\begin{aligned} V_k(V_k - V_j) &= (1 + \Delta V_k)(1 + \Delta V_k - 1 - \Delta V_j) \\ &= (1 + \Delta V_k)(\Delta V_k - \Delta V_j)\Delta V_k \\ &\quad + \Delta V_k^2 - \Delta V_j - \Delta V_k \Delta V_j \end{aligned} \quad (3)$$

From (3), the second step ΔV_k^2 and $\Delta V_k \Delta V_j$ can be neglected without causing high errors as they are a second order of a small magnitude that is smaller than V_k and V_j.

$$V_k(V_k - V_j) \approx (\Delta V_k - \Delta V_j) \approx (V_k - V_j) \quad (4)$$

Taking these assumptions into account, equations (1) and (2) are reorganized in a matrix structure after being

linearized as follows:

$$\begin{bmatrix} P^A \\ P^B \\ P^C \\ Q^A \\ Q^B \\ Q^C \end{bmatrix} = \begin{bmatrix} J_{PV}^{AA} & J_{PV}^{AB} & J_{PV}^{AC} & J_{P\theta}^{AA} & J_{P\theta}^{AB} & J_{P\theta}^{AC} \\ J_{PV}^{BA} & J_{PV}^{BB} & J_{PV}^{BC} & J_{P\theta}^{BA} & J_{P\theta}^{BB} & J_{P\theta}^{BC} \\ J_{PV}^{CA} & J_{PV}^{CB} & J_{PV}^{CC} & J_{P\theta}^{CA} & J_{P\theta}^{CB} & J_{P\theta}^{CC} \\ J_{QV}^{AA} & J_{QV}^{AB} & J_{QV}^{AC} & J_{Q\theta}^{AA} & J_{Q\theta}^{AB} & J_{Q\theta}^{AC} \\ J_{QV}^{BA} & J_{QV}^{BB} & J_{QV}^{BC} & J_{Q\theta}^{BA} & J_{Q\theta}^{BB} & J_{Q\theta}^{BC} \\ J_{QV}^{CA} & J_{QV}^{CB} & J_{QV}^{CC} & J_{Q\theta}^{CA} & J_{Q\theta}^{CB} & J_{Q\theta}^{CC} \end{bmatrix} \begin{bmatrix} V^A \\ V^B \\ V^C \\ \theta^A \\ \theta^B \\ \theta^C \end{bmatrix} \tag{5}$$

Equation (5) represents again the real and reactive power injected in each phase and bus. The J-matrix is an N×N size, where N is the number of buses multiplied by 3 (the number of phases in each bus), and it exclusively depends on the system's impedance. Hence, it should be calculated once, assuming no system reconfiguration occurs. Solving equation (5) will determine all injected real and reactive powers for all buses and all phases. The following relationships illustrate three items from this matrix:

$$J_{QV}^{AA} = -B^{AA} \tag{6}$$

$$J_{PT}^{CA} = -((-\sqrt{3}/2) * G^{CA} + (-1/2) * B^{CA}) \tag{7}$$

$$J_{QV}^{CB} = ((-\sqrt{3}/2) * G^{CB} + (1/2) * B^{CB}) \tag{8}$$

The next step involves determining the power transferred between each pair of connected buses k and j. To calculate these power values, the nonlinear power flow formula for phase A, as shown in (9), is utilized. By applying the previous two assumptions, this formula is transformed into a linear form for the power flow in each branch, as indicated in (10) [35]. In this context, r_{kj}^A and x_{kj}^A represent the resistance and reactance of branch kj, respectively. This formula is consistently applied across all phases in the system. It is important to note that the linearization of the nonlinear DN model is based on the assumption that losses are negligible, assuming that the power flow from one bus to another remains constant. The practice of overlooking losses in the linear model of the DN is commonly adopted in DN planning, as evidenced in several studies, for example, [36], [37], and [38].

$$P_{kj}^A = \frac{r_{kj}^A V_k^{A^2} - r_{kj}^A V_k^A V_j^A Cos\theta_{kj}^A + x_{kj}^A V_k^A V_j^A Sin\theta_{kj}^A}{r_{kj}^{A^2} + x_{kj}^{A^2}} \tag{9}$$

$$P_{kj}^A \simeq \frac{r_{kj}^A x_{kj}^A}{r_{kj}^{A^2} + x_{kj}^{A^2}} \frac{V_k^A - V_j^A}{x_{kj}^A} + \frac{x_{kj}^{A^2}}{r_{kj}^{A^2} + x_{kj}^{A^2}} \frac{\theta_k^A - \theta_j^A}{x_{kj}^A} \tag{10}$$

III. PROBLEM FORMULATION

The proposed planning optimization model aims to maximize the total payoffs of the EVA by participating in energy and AS markets during the studied period. The proposed model considers the general case where the DN is unbalanced. This section details the optimization's objective function and constraints.

A. OBJECTIVE FUNCTION FORMULATION

The planning objective function is formulated and developed as follows:

$$TP = \sum_{y=1}^{NY} (1+r)^{-y}.OpP_y - InvC \tag{11}$$

$$InvC = \sum_{i=1}^{NEV} (SC + ComC + BiC.MP_i) \tag{12}$$

$$OpP_y = \sum_{W=1}^{NW} \sum_{d=1}^{7} (OpI_{dw} - OpC_{dw}) \tag{13}$$

$$OpI_{dw} = \sum_{t=1}^{T} \omega_{tdw}.(\sigma_{tdw}^D R_{tdw}^D + \sigma_{tdw}^U R_{tdw}^U + \sigma_{tdw}^R R_{tdw}^R) + \beta \sum_{t=1}^{T} \omega_{tdw} \sum_{e=1}^{NEV} E[FP_{etdw}] \tag{14}$$

$$OpC_{dw} = \sum_{t=1}^{T} \omega_{tdw} \sum_{e=1}^{NEV} \sigma_{tdw}^E E[FP_{etdw}] + \sum_{t=1}^{T} \sum_{e=1}^{NEV} g_{etdw} \tag{15}$$

$$R_{tdw}^D = \sum_{e=1}^{NEV} AP_{etdw}^D \tag{16}$$

$$R_{tdw}^U = \sum_{e=1}^{NEV} AP_{etdw}^U \tag{17}$$

$$R_{tdw}^R = \sum_{e=1}^{NEV} AP_{etdw}^R \tag{18}$$

The objective function aims to maximize the total profits (TP), considering the discount rate (r), as outlined in (11). This function comprises two components: The first is the operational profits (OpP_y) accumulated over the year, and the second is the investment cost ($InvC$), which is relevant only in the first year.

The $InvC$ and OpP_y are computed according to (12) and (13), respectively. The $InvC$ includes infrastructure cost (SC) and communication cost ($ComC$), as illustrated in (12). The MP in (12) denotes the EV battery's maximum power capacity, varying based on the EV model; for instance, the Nissan Leaf features a 2 kW inverter. The OpP_y, as specified in (13), is calculated by deducting the daily costs (OpC_{dw}) from the daily incomes (OpI_{dw}), whereas OpI_{dw} and OpC_{dw} are calculated in (14) and (15), respectively. $E[FP_{etdw}]$ can be either positive or negative. In case of a negative value, it is interpreted as selling energy to the market, so it contributes to a negative cost as stated in (15). Conversely, in case the value is positive, it is considered as buying from the energy market. The subscripts t, d, and w represent hour, day, and week, respectively. The OpI_{dw} is derived from participation in the AS market, through bidding on regulation up (R_{tdw}^U), regulation down (R_{tdw}^D) and reserve capacity (R_{tdw}^R) with AS prices σ_{tdw}^D, σ_{tdw}^U and σ_{tdw}^R for regulation up, regulation down and reserve capacity, respectively. It also includes revenue from selling energy to EV owners at a fixed tariff (β),

multiplied by the expected power draw ($E[FP_{etdw}]$) of all EVs. The OpC_{dw} is calculated based on the cost of purchasing energy from the grid at the market price (σ^{E}_{tdw}) and the degradation cost (g_{etdw}) associated with the reduced lifespan of EV batteries during the discharging process. The total bidding capacity at each time interval is the cumulative capacity of all EVs, applicable to R^{D}_{tdw}, R^{U}_{tdw} and R^{R}_{tdw}, as demonstrated in (16), (17), and (18). Here, AP^{U}_{etdw}, AP^{D}_{etdw}, and AP^{R}_{etdw} represent the capacities for regulation up, down, and reserve, respectively.

$$E[FP_{etdw}] = (POP_{etdw+} + \alpha^{D}_{etdw}AP^{D}_{etdw} - \alpha^{U}_{etdw}AP^{U}_{etdw} - \alpha^{R}_{etdw}AP^{R}_{etdw})v_{etdw} \quad (19)$$

$$\omega_{tdw} = 1 - (1/NEV)\sum_{e=1}^{NEV}\pi^{A}_{etdw} \quad (20)$$

$$\pi^{A}_{etdw} = \sum_{h=\tau^{p-1}_{e}}^{t}\pi^{A}_{ehdw},\ \tau^{p}_{e} \le t < \tau^{p-1}_{e} \quad (21)$$

where $\tau^{0}_{e} = 1, p = 1, 2, \ldots, NP$

$$SOC_{etdw} = SOC_{e,t-1dw} + E[FP_{etdw}]\delta_{edw}\eta_{e} - E_{etdw} \quad (22)$$

$$g_{etdw} = max(\frac{-DC_{e}E[FP^{-}_{etdw}]\delta_{edw}}{\eta_{e}}, 0) \quad (23)$$

$$E[FP^{-}_{etdw}] = (POP_{etdw} - \alpha^{U}_{etdw}AP^{U}_{etdw} - \alpha^{R}_{etdw}AP^{R}_{etdw})v_{et} \quad (24)$$

$$DC_{e} = 0.042\left(\frac{BatC}{312}\right) + \frac{\beta(1-\eta^{2}_{e})}{\eta_{e}} \quad (25)$$

$$\delta_{etdw} = (1 - \pi_{etdw})^{-1} \quad (26)$$

The $E[FP_{etdw}]$ is calculated as per (19). It functions based on the POP_{etdw} and is influenced by the expected bidding capacities AP^{U}_{etdw}, AP^{D}_{etdw} and reserve AP^{R}_{etdw}, which are decision variables. The signals α^{U}_{etdw}, α^{D}_{etdw}, α^{R}_{etdw} represent regulation up, regulation down, and reserve, respectively, and are received from the ISO to determine the proportion of bidding capacities provided by the EVA. The sign of $E[FP_{etdw}]$ indicates whether the EV is injecting or consuming power: a negative value means power injection into the DN, while a positive value indicates power draw from the DN.

Every participating EV follows a simulated daily commute profile, including two random weekend journey times and regular weekday morning and evening trips, with departures expected around the same time each day. The variable v_{et} takes values 0 or 1, depending on the trip profile of each EV. For instance, if v_{et} is 0, meaning the EV is not connected to the charger, the EVA cannot utilize this EV for providing AS. As a result, $E[FP_{etdw}]$ will be 0, indicating no power draw or injection at that specific hour t. Each EV has a probability of an unexpected departure, making it unavailable for a certain number of hours. Therefore, the percentage availability of EVs to provide AS is represented by ω_{t} and it is calculated as shown in (20). This depends on the departure probability (π^{A}_{et}) at time t, calculated in (21). Both OpI_{dw} and OpC_{dw} are dependent on the probability of unexpected departure (π^{A}_{et}) and the availability (ω_{t}) of each EV. After each trip, π^{A}_{et} resets to zero due to the certainty of EV availability at this time. The total numbers of scheduled trips during the day is represented by NP. If there are two trips, the first trip is at τ^{p-1}_{e} and the second trip is at τ^{p}_{e}. π^{A}_{et} is calculated in the period when $\tau^{p-1}_{e} < t < \tau^{p}_{e}$, where $t < \tau^{p-1}_{e}$ and $t > \tau^{p}_{e}$ as in relation (21). The state of charge (SOC_{t}) is defined in (22), where E_{et} is the energy consumed during the trip and $SOC_{e,t-1}$ is the previous state of the battery. As illustrated in (22), $E[FP_{etdw}]$ is multiplied by two parameters. The first parameter is the efficiency (η_{e}) of charging/discharging EV battery, which depends on the bi-directional inverter. The second parameter is the compensation factor (δ_{et}), which equals 1 when EV is available and less than 1 when there is a possibility for unexpected departure based on (26).

The degradation cost (g_{etdw}) due to EV battery discharging is calculated as per equations (23), (24), and (25) and is represented as a positive cost. The formula for g_{etdw} is the maximum of 0 and $\frac{-DC_{e}E[FP^{-}_{etdw}]\delta_{et}}{\eta_{e}}$. When the EV is charging, $E[FP^{-}_{etdw}]$ is positive, resulting in g_{etdw} being zero, indicating no battery lifespan reduction. Conversely, during discharging, $E[FP^{-}_{etdw}]$ is negative, leading to a positive degradation cost calculated due to the battery lifespan reduction. The term (DC) represents the cost of deregulation per kWh where the term $BatC/312$ is used to normalize the deregulation cost by $312\$/kWh$ in [39]. The second term is the cost of the lost energy due to cycling, as developed in [40]. As shown in (24), the degradation cost is affected by the regulation up (AP^{U}_{tdw}) and the reserve (AP^{R}_{tdw}). The compensation factors for unexpected departures are calculated as in (26).

B. CONSTRAINTS

$$\varphi_{e}MC_{e} \le SOC_{et} \le MC_{e}, \forall t \le T-1 \quad (27)$$

$$\varphi_{e}MC_{e} \le SOC_{et} \le MC_{e} \quad (28)$$

$$(POP_{etdw} + AP^{D}_{etdw})\delta_{et}\eta_{e} \le MC_{e} - SOC_{et} \quad (29)$$

$$(POP_{etdw} - AP^{U}_{etdw} - AP^{R}_{etdw})\delta_{et}\eta_{e} + SOC_{et} \ge E_{et} \quad (30)$$

$$(POP_{etdw} + AP^{D}_{etdw})\delta_{et} \le MP_{e}v_{et} \quad (31)$$

$$POP_{etdw} - AP^{U}_{etdw} - AP^{R}_{etdw} \ge -v_{et}MP_{e} \quad (32)$$

$$AP^{D}_{etdw}, AP^{U}_{etdw}, AP^{R}_{etdw} \ge 0 \quad (33)$$

$$POP_{etdw} \ge -v_{et}MP_{e} \quad (34)$$

$$\left|SOC_{etdw} - SOC_{e,t-1,d,w}\right| \le v_{et}MP_{e}/\eta_{e} \quad (35)$$

Inequality constraint (27) ensures that the SOC_{et} of the EV battery operates within the energy capacity (MC_{e}) and remains above a certain limit to protect the battery from deep discharging. Relation (28) is implemented to guarantee that the SOC_{t} of the EV is within an acceptable range at the start of each day, enabling the EV owner to embark on daily trips. Constraints (29) and (30) link the energy limit of the battery for each EV with the decision variables of the AS bid capacities and the POP. These constraints are essential for ensuring that the EV's battery has sufficient energy available

in real time, in case its full capacity is needed. Relation (30) limits regulation up and reserve capacities, while relation (29) limits the regulation down capacity. Constraints (31), (32), (34), and (35) address the capacity of the power inverter, where MP_e correlates this capacity with the decision variable. Specifically, relation (35) ensures that performing regulation up or down at any moment does not exceed the power capacity of the inverter. This optimization problem encompasses six decision variables: β, POP_{tdw}, AP^U_{tdw}, AP^D_{tdw} and AP^R_{tdw}.

C. INTEGRATING DISTRIBUTION NETWORK MODEL WITH EV PLANNING MODEL

To integrate the EVS model with the unbalanced DN model, the total number of EVs to be analyzed is distributed across the DN. Consequently, each bus in the system accommodates a certain number of EVs. When power is drawn from the grid to charge EVs at bus k, this power is considered as a load. Conversely, when power is injected into the grid from the EV batteries, it is considered as a negative load.

$$Power^k_{tdw} = \begin{cases} POP^k_{tdw} + APD^k_{tdw} & (a) \\ POP^k_{tdw} - APU^k_{tdw} + APR^k_{tdw} & (b) \end{cases} \quad (36)$$

$$\left|LF^{\alpha}_{kj}\right| \leq LF^{max}_{kj} \quad (37)$$

$$V_{min} \leq V^{\alpha}_{k} \leq V_{max} \quad (38)$$

$$\theta_{min} \leq \theta^{\alpha}_{k} \leq \theta_{max} \quad (39)$$

In this study, EVs are assumed to consume or inject real power only. As depicted in Figure 2, there are two extreme scenarios for the power injected or consumed by EVs. The first scenario occurs when the EVS is requested to provide full regulation down capacity $\left(APD^k_{tdw}\right)$ and no regulation up or reserve $\left(APU^k_{tdw}, APR^k_{tdw}\right)$. In this case, the EV will consume high power from the DN depending on the POP, as described in (36-a). The second scenario arises when the EVA is requested to provide full regulation up and reserve $\left(APU^k_{tdw}, APR^k_{tdw}\right)$ and no regulation down $\left(APD^k_{tdw}\right)$. Here, the EV will inject a significant amount of power into the DN, as indicated in (36-b). In both scenarios (36 a and b), DN limitations should not be exceeded. When the variable $\left(Power^k_{tdw}\right)$ is negative, it is considered as a negative load. Relation (37) limits the maximum power transfer between buses k and j. The inequalities (38) and (39) limit the voltage magnitude and angle to values deemed acceptable by the ISO.

D. COMPLETE EVA PLANNING MODEL

The full optimization model of EVA (11)-(35) integrated with the distribution model (5), (36)-(39) is solved to maximized the aggregator's profits. This planning problem has two sets of decision variables. The first set is the most important, including the number of EVs in the fleet participating in AS (γ) and the energy tariff paid by the EV owners to the EVA (β). The second set is the operational and network decision variables POP, AP^D, AP^U, AP^R, LF and V.

IV. CASE STUDY

This case study aims to evaluate the profitability of EVA investment in providing AS, as well as the implications of incorporating an unbalanced DN into the final decisions. The project is assumed to have a lifespan of 12 years with a 5% discount rate. The selected period of 12 years aligns with the average lifetime of light-duty vehicles in the USA. Although the current lifespan of Li-ion batteries is somewhat shorter, it is expected to reach this duration with the aid of an efficient management system [41]. The costs for maintenance and installation are incorporated into the energy and power costs, set at 190\$/kW and 200\$/kW for the power and energy capacities, respectively [41]. The efficiency of the bi-directional inverter is assumed to be 90% for both charging and discharging processes.

This study is assumed to be in Houston, Texas, with an estimated 70,000 EVs in the mix (50% Nissan Leaf, 20% Mitsubishi i-MiEVs, and 30% Tesla Model S). These EVs are assumed to follow one of the 100 trip profiles derived from actual EV usage in Houston. The simulated data for AS (regulation up/down and reserves), energy prices, and the AS deployment signals are sourced from the ERCOT market data [31]. Average price trends for a typical day are depicted in Figure 3.

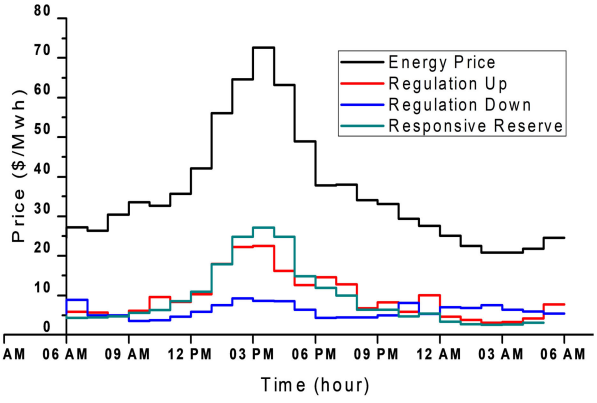

FIGURE 3. Average prices during the day.

To test the proposed model, the IEEE 13 bus unbalanced DN is utilized. For simplicity, all transformers and voltage regulators have been omitted. Additionally, EVs are assumed to inject or draw real power only, allowing for the omission of reactive power due to its relatively small amount compared to real power. Figure 4 illustrates the system and indicates the peak load for each phase (A, B, C) at each bus in kW. As depicted in Figure 4, some phases are available only in certain buses, reflecting the unbalanced nature of the DN. References [42] and [43] provide comprehensive details about the DN. To enhance the model's realism, minor modifications are made by generating random load profiles from two categories of loads (household and commercial). This is achieved by adding random errors to two base profiles, which are then distributed among the various buses [44] in the DN, ensuring that each phase at a bus has a various

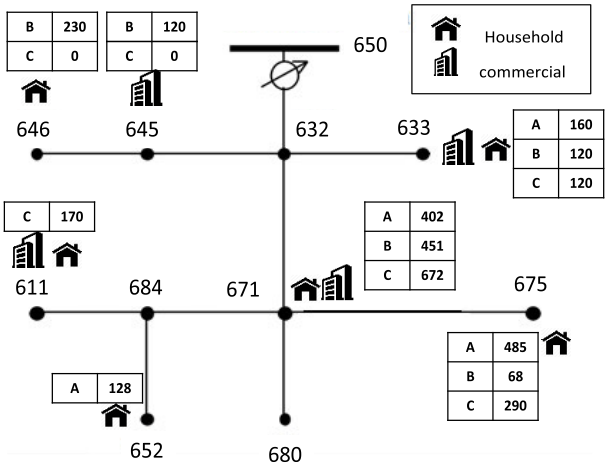

FIGURE 4. One-line diagram of the IEEE 13 unbalanced radial bus system with the peak load of each bus in kW.

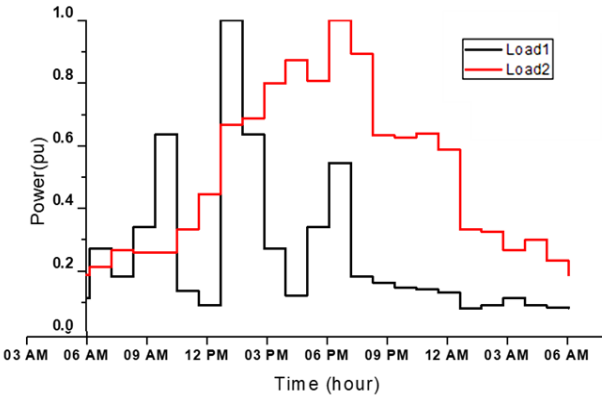

FIGURE 5. Normalized load profiles for one day.

load profile. Figure 5 displays two normalized load profiles for a typical day. All lines in the system are designed with a line thermal capacity of 700 kVA, except for the main line connecting bus 632 with 671, which has a higher thermal limit of 1400 kVA.

The primary outcomes of this planning optimization are the energy tariff charged to the customer (β) ($\$/kWh$), and the total profits (TP) over the period under study. The percentage of EV participation in AS is contingent on β, which varies from a minimum of $\beta_{min} = 0$ to a maximum of $\beta_{max} = 0.12\$/kwh$. No EVs will participate at $\beta = 0.12$; for intermediate values, linear relationships with varying

TABLE 1. Parameters and constants.

Parameter	Value	Parameter	Value
r	5%	NT	70,000
NEV	100 EVs	T	24 h
NY	12 Years	BiC	$186.7\$/kw$
NW	52 Weeks	η	0.9
φ	0.1	ϕ	0.99
ComC	$88.4\$/kw$	ChC	$186.7\$/kw$
SC	$36.1\$/kw$		

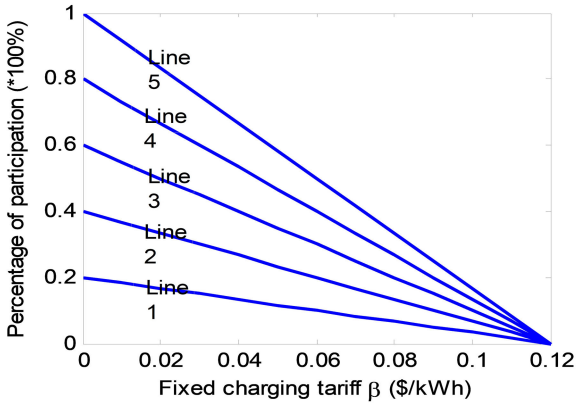

FIGURE 6. The relation between β and the EVs participant$\gamma = 0.2, 0.4, 0.6, 0.8$, and 1.

slopes are assumed, as illustrated in Figure 6. As indicated in equation (14), β interacts with other decision variables (POP, AP^D, AP^U, AP^R), rendering the problem nonlinear. An iterative approach is employed to address this complexity, incrementing β by 0.01 within the range of 0 to $\$/kWh$. Figure 7 presents a flow chart detailing the optimization process.

V. RESULTS

A. RESULTS WITHOUT CONSIDERING DN

In this sub-section, the result of the EVA planning is obtained by solving equations (11)-(35) and disregarding the unbalanced DN model.

This section will provide results for two cases as follows:

1) The EVs are scheduled for two one-hour trips each day: one in the morning and one in the evening. Outside of these two hours, the EVs are assumed to be available and connected to a charger for the rest of the day. This trip schedule aligns with the proposals in several literature review papers, such as [20], [45], and [46]. The investment cost calculations assume that each EV is equipped with a home charger. The EV is expected to leave and return home at each trip hour.
2) The EV is not available between the two trips, and the investment cost remains consistent with the first case. This approach is more realistic of a typical daily routine, where the EV is used for commuting to work in the morning and returning in the evening. Since the investment cost is only allocated for installing a home charger, the EV is unavailable during the workday.

In the first case, Figure 8 illustrates the optimal profits for line 3, with a 60%($\gamma = 0.6$)) participation rate, when β is incremented by 0.01 within the range of 0 to 0.1 $\$/kWh$. The highest payoffs are observed when β is set to 0, which corresponds to a 60% participation of the total 70,000 EVs. This indicates that the profits derived from AS participation outweigh those from charging the EVs, prompting the EVA to maximize EV participation by setting β to 0. This outcome is anticipated, given the relatively low consumption of EVs

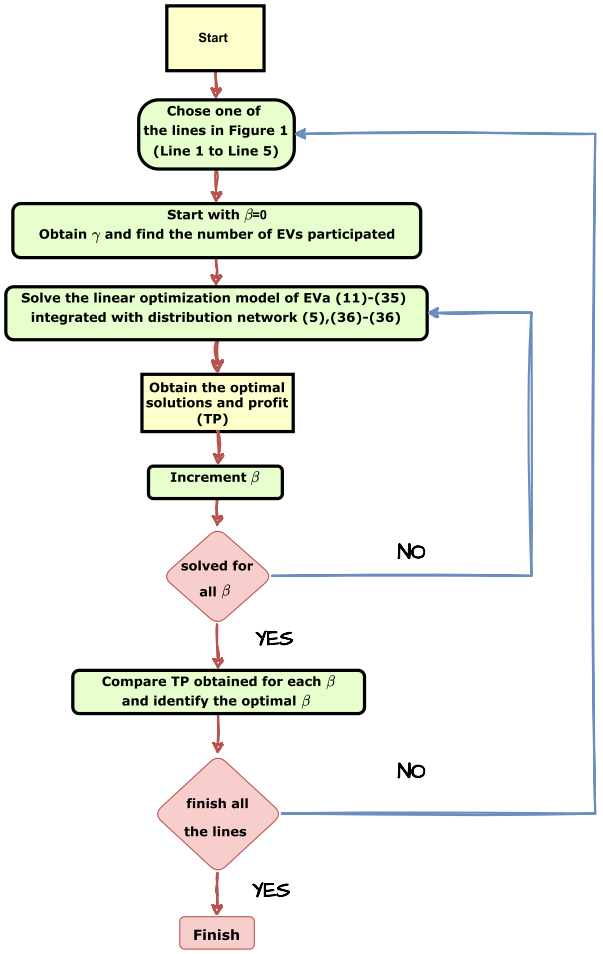

FIGURE 7. Optimization process.

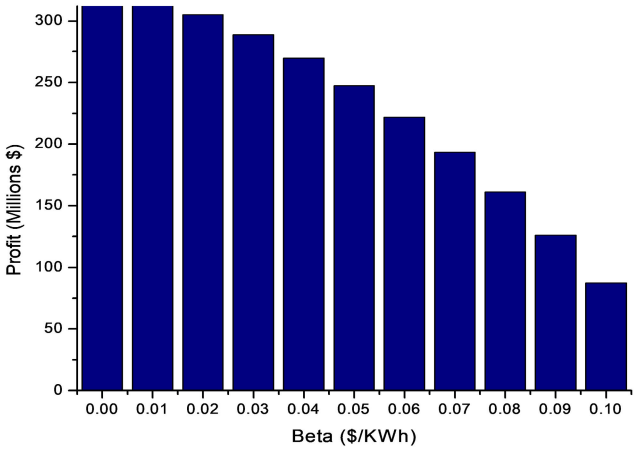

FIGURE 8. EVA Profits versus β for line 3 with a participation of 60% ($\gamma = 0.6$) case one.

TABLE 2. EVA optimal decision for the first case.

Line	Investment cost (Millions$)	Fixed charging tariff $\beta(\$/kWh)$	Percentage of participation (γ)	EV Aggregator Payoff (Millions$)
$1(\gamma = 0.2)$	23.46	0	20%	109.3
$2(\gamma = 0.4)$	46.92	0	40%	218.6
$3(\gamma = 0.6)$	70.38	0	60%	327.9
$4(\gamma = 0.8)$	93.84	0	80%	437.2
$5(\gamma = 1)$	117.3	0	100%	546.9

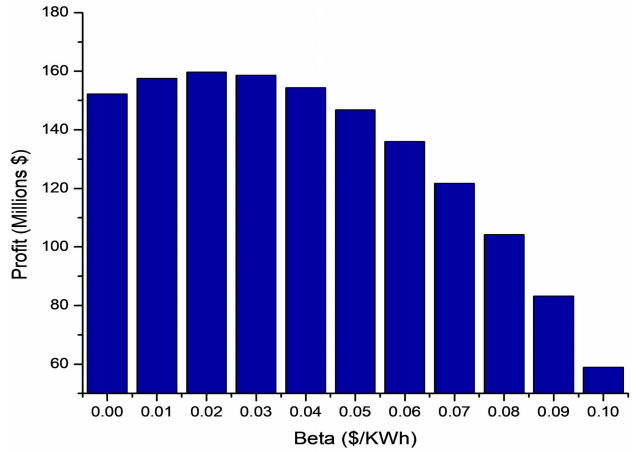

FIGURE 9. EVA Profits versus β for line 3 with a participation of 60% ($\gamma = 0.6$) case two.

in this scenario, leading to limited profits from charging. As a result, utilizing the EV's battery, which is available for 22 hours a day for AS, proves to be more profitable. Table 2 presents the optimal profits for the five lines ($\gamma = 0.2, 0.4, 0.6, 0.8, 1$), all occurring when β equals 0. The results for the other four lines mirror the trend shown in Figure 8.

For the second case, when EVs here are unavailable between the two trips, Figure 9 shows the optimal EVA payoffs. The optimal profits happen when β equals $0.02\$/kWh$. EVs are unavailable between trips, reducing the profits from AS participation and forcing the EVA to increase β to get profits from charging the EVs. Table 3 shows the optimal profits for the other lines at β equals $0.02\$/kWh$.

Figure 10 compares the first and second cases. In addition to the shift of the optimal β to $0.02\$/kWh$, it is clear that the total profits are reduced by about 50% when the EVs are not available between the trips.

B. RESULTS WITH CONSIDERING DN

In this section, the results of integrating the EV model with an unbalanced DN (specifically, the IEEE 13 bus system) are presented. As discussed in the case study, there are 70,000 EVs available. However, due to the DN's limited size, accommodating this large number proved infeasible. To address this challenge, the optimal investment cost for BESS of approximately 5.47 million dollars, as presented in [47], is adopted as the investment cost for the EVA. This investment cost allows for the estimation of the total number of EVs in the network using equation (12), resulting in a calculated figure of 3,500 EVs. The results are then scaled

TABLE 3. EVA optimal decision for the second case.

Line	Investment cost (Millions$)	Fixed charging tariff $\beta(\$/kWh)$	Percentage of participation (γ)	EV Aggregator Payoff (Millions$)
$1(\gamma = 0.2)$	19.55	0.02	16.67%	53.23
$2(\gamma = 0.4)$	39.11	0.02	33.33%	106.46
$3(\gamma = 0.6)$	58.66	0.02	50.00%	159.70
$4(\gamma = 0.8)$	78.21	0.02	66.67%	212.92
$5(\gamma = 1)$	97.76	0.02	83.33%	266.15

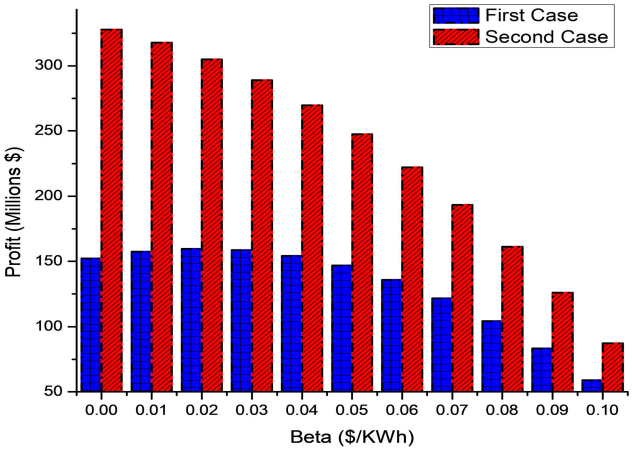

FIGURE 10. EVA Profits versus β for line 3 with a participation of 60% ($\gamma = 0.6$) case one and two.

FIGURE 11. EVs distribution in the DN.

up by a factor of 20 to represent the total number of EVs. This number is presumed to be evenly distributed across the different buses in the system, as illustrated in Figure 11. Only the second scenario, where EVs are unavailable during the period between the two trips, is considered, as this approach is deemed more realistic based on previous descriptions.

Figure 12 shows the optimal profits along with the investment cost for line 3 (participation of 60% ($\gamma = 0.6$)). As seen, the optimal profits of 122 million occurred when β is 0.05 $\$/kWh$ and required an investment cost of 42 million. That corresponds to 35% (24500 EVs) participants. The aggregator here tried to attract a smaller number of EVs due to the network voltage and line constraints to bid higher capacities to AS market without exceeding those limits.

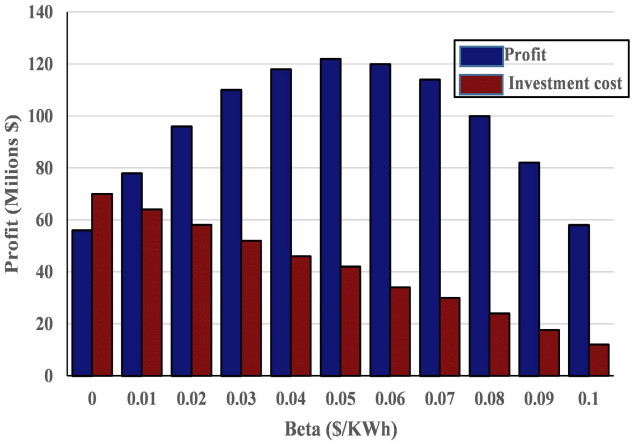

FIGURE 12. EVA profits along with investment cost versus β for line 3 with a participation of 60% ($\gamma = 0.6$) in DN.

TABLE 4. EVA optimal decision for including DN.

Line	Investment cost (Millions$)	Fixed charging tariff $\beta(\$/kWh)$	Percentage of EVs participated	EV Aggregator Payoff (Millions$)
$1(\gamma = 0.2)$	19.55	0.02	16.67%	52
$2(\gamma = 0.4)$	31.20	0.04	26.66%	93
$3(\gamma = 0.6)$	42	0.05	35%	122
$4(\gamma = 0.8)$	47	0.06	40%	145
$5(\gamma = 1)$	58.66	0.06	50%	163.4

Table 4 shows that the optimal decision depends mainly on the relation between β and the number of EVs participating. When the slope of the relationship increases, the optimal β also increases. From that, we can conclude that the availability of more EVs in the system restricts the EVA from bidding capacities to AS market due to the thermal and voltage limits, which cause the increase in the energy tariff β. Thus, the EVA will try to get more profits from charging EVs than participating in AS market by attracting fewer EVs by increasing β to attract fewer EVs.

In the previous cases, the EVs are assumed to be distributed equally in the DN, as shown in Figure 11. The distribution of EVs will be changed so that EVs are in 633, 646, and 671, as shown in Figure 13. Those buses are chosen because, in the BESS optimization, most of the capacities are located there [47].

Table 5 summarizes the results of all lines. The optimal aggregator payoff for all lines is slightly less than in the previous case, where EVs are distributed across the buses equally. To illustrate, the additional loads of EVs placed on one bus could highly cause overloading of those buses and exceed the thermal limits of the line. Interestingly, the optimal β is the same for all lines, as in Table 5.

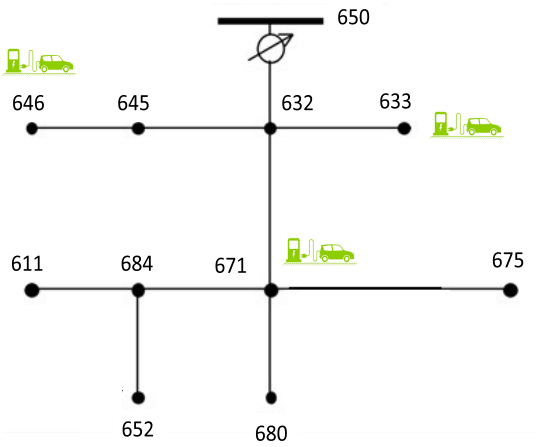

FIGURE 13. EVs distribution in the DN (633, 646 and 671).

TABLE 5. EVA optimal decision for including DN when EVs in 633, 646 and 671.

Line	Investment cost (Millions$)	Fixed charging tariff $\beta(\$/kWh)$	Percentage of EVs participated	EV Aggregator Payoff (Millions$)
$1(\gamma = 0.2)$	19.55	0.02	16.67%	44
$2(\gamma = 0.4)$	31.20	0.04	26.66%	91.6
$3(\gamma = 0.6)$	42	0.05	35%	118
$4(\gamma = 0.8)$	47	0.06	40%	140.6
$5(\gamma = 1)$	58.66	0.06	50%	161.4

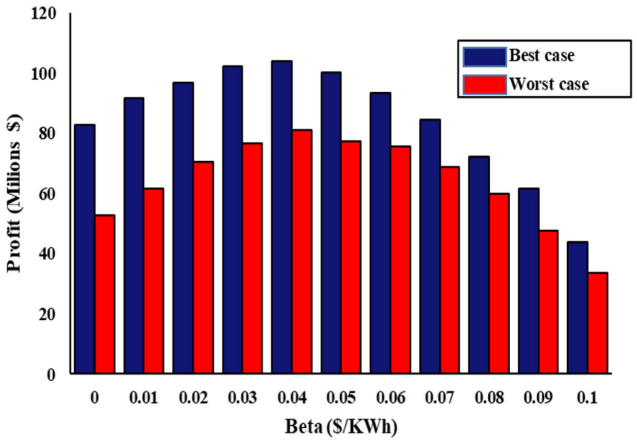

FIGURE 14. EVA profits for the two cases versus β for line 2 with a participation of 40% ($\gamma = 0.4$) in DN.

C. EFFECT OF UNCERTAINTIES IN PRICES

In this section, we explore the impact of a 10% uncertainty in energy and ancillary services (AS) prices ($\sigma^{D,U,R}$, σ^{E}). This section is done based on $\gamma = 0.4$ with the same parameters and assumption used in Table 5. We delve into two distinct cases to comprehensively analyze their implications:

1) In the worst-case scenario, AS prices deviate negatively by 10% from expectations, while energy prices register an increase of 10%.
2) In the best-case scenario, AS prices deviate positively by 10% from expectations, while energy prices register a decrease of 10%.

The results of both cases are shown in Figure 14. In the worst-case scenario, the optimal payoffs drop by 11.6% from 91.6 million (Table 5) to 80.96 million. On the other hand, in the best-case scenario, the optimal payoffs increase by 13.36% from 91.6 million (Table 5) to 103.84 million. for both cases, the optimal charging tariff β remains the same at 0.04 ($\$/kWh$).

VI. CONCLUSION

This work investigates the investment potential of utilizing EV batteries in a fleet coordinated by an EVA for bidding regulation and reserve capacities in the AS market. A linear planning model for the EVA was developed and integrated with an unbalanced DN to optimize long-term profits and determine the optimal bidding and charging tariffs during the studied period.

The employed model revealed various profit margins when including versus disregarding the DN. Additionally, the placement of EVs within the DN significantly influences the optimal payoff. The key findings are summarized as follows:

1) When the DN is disregarded, optimal payoffs are achieved when the charging tariff (β) is set to 0 ($\$/kWh$), assuming EV availability throughout the day except for two trip hours. Due to higher profits from AS participation, which surpass profits from charging EVs and the absence of DN limitations, the EVA aims to attract the maximum number of EVs to increase AS bids to the market. However, when EVs are unavailable between trips, reduced AS participation profits compel the EVA to raise β to 0.02 ($\$/kWh$) to gain revenue from charging EVs and attract fewer EVs.
2) Including the DN, optimal payoffs are achieved at varying values depending on the correlation between the charging tariff and the number of participating EVs, such as 0.05 ($\$/kWh$) for line 3 as shown in Figure 6. The presence of additional EVs in the DN limits the EVA's capacity to bid in the AS market due to thermal and voltage constraints, leading to increased energy tariffs. Consequently, the EVA focuses on maximizing profits from charging EVs over AS market participation, attracting fewer EVs to remain within DN constraints.
3) The optimal charging tariff (β) remains consistent whether EVs are selectively distributed among specific buses (targeting critical buses) or evenly distributed across the DN.

REFERENCES

[1] *Annual Energy Review*, U.S. Energy Inf. Admin. (EIA), 2011. Accessed on: Feb. 21, 2024. [Online]. Available: https://www.eia.gov/totalenergy/data/annual/pdf/aer.pdf
[2] CEIC Data. *Saudi Arabia Environmental Energy Production and Consumption: Non-OECD Member: Annual*. Accessed: Jan. 12, 2024. [Online]. Available: https://www.ceicdata.com

[3] B. Mohandes, M. S. E. Moursi, N. Hatziargyriou, and S. E. Khatib, "A review of power system flexibility with high penetration of renewables," *IEEE Trans. Power Syst.*, vol. 34, no. 4, pp. 3140–3155, Jul. 2019.

[4] A. J. Headley and D. A. Copp, "Energy storage sizing for grid compatibility of intermittent renewable resources: A California case study," *Energy*, vol. 198, May 2020, Art. no. 117310.

[5] B. Nykvist and M. Nilsson, "Rapidly falling costs of battery packs for electric vehicles," *Nature Climate Change*, vol. 5, no. 4, pp. 329–332, Apr. 2015.

[6] A. Ford, "Electric vehicles and the electric utility company," *Energy Policy*, vol. 22, no. 7, pp. 555–570, Jul. 1994.

[7] A. N. Brooks, "Vehicle-to-grid demonstration project: Grid regulation ancillary service with a battery electric vehicle," California Air Resour. Board Environ. Protection Agency, CA, USA, Final Rep., 2002. [Online]. Available: https://heritageproject.caltech.edu/documents/21133/Carb_V2G_project_final_report_emlP1Xu.pdf

[8] J. J. Escudero-Garzas, A. Garcia-Armada, and G. Seco-Granados, "Fair design of plug-in electric vehicles aggregator for V2G regulation," *IEEE Trans. Veh. Technol.*, vol. 61, no. 8, pp. 3406–3419, Oct. 2012.

[9] T. N. Pham, H. Trinh, and L. V. Hien, "Load frequency control of power systems with electric vehicles and diverse transmission links using distributed functional observers," *IEEE Trans. Smart Grid*, vol. 7, no. 1, pp. 238–252, Jan. 2016.

[10] C. Shao, X. Wang, X. Wang, C. Du, and B. Wang, "Hierarchical charge control of large populations of EVs," *IEEE Trans. Smart Grid*, vol. 7, no. 2, pp. 1147–1155, Mar. 2016.

[11] K. Knezovic, S. Martinenas, P. B. Andersen, A. Zecchino, and M. Marinelli, "Enhancing the role of electric vehicles in the power grid: Field validation of multiple ancillary services," *IEEE Trans. Transport. Electrific.*, vol. 3, no. 1, pp. 201–209, Mar. 2017.

[12] J. Meng, Y. Mu, H. Jia, J. Wu, X. Yu, and B. Qu, "Dynamic frequency response from electric vehicles considering travelling behavior in the great Britain power system," *Appl. Energy*, vol. 162, pp. 966–979, Jan. 2016.

[13] H. Liu, Z. Hu, Y. Song, and J. Lin, "Decentralized vehicle-to-grid control for primary frequency regulation considering charging demands," *IEEE Trans. Power Syst.*, vol. 28, no. 3, pp. 3480–3489, Aug. 2013.

[14] E. Yao, V. W. S. Wong, and R. Schober, "Robust frequency regulation capacity scheduling algorithm for electric vehicles," *IEEE Trans. Smart Grid*, vol. 8, no. 2, pp. 984–997, Mar. 2017.

[15] E. Yao, V. W. S. Wong, and R. Schober, "Optimization of aggregate capacity of PEVs for frequency regulation service in day-ahead market," *IEEE Trans. Smart Grid*, vol. 9, no. 4, pp. 3519–3529, Jul. 2018.

[16] S. Cai and R. Matsuhashi, "Model predictive control for EV aggregators participating in system frequency regulation market," *IEEE Access*, vol. 9, pp. 80763–80771, 2021.

[17] X. Chen and K.-C. Leung, "Non-cooperative and cooperative optimization of scheduling with vehicle-to-grid regulation services," *IEEE Trans. Veh. Technol.*, vol. 69, no. 1, pp. 114–130, Jan. 2020.

[18] H. Nakano, I. Nawata, S. Inagaki, A. Kawashima, T. Suzuki, A. Ito, and W. Kempton, "Aggregation of V2H systems to participate in regulation market," *IEEE Trans. Autom. Sci. Eng.*, vol. 18, no. 2, pp. 668–680, Apr. 2021.

[19] E. Sortomme and M. A. El-Sharkawi, "Optimal charging strategies for unidirectional vehicle-to-grid," *IEEE Trans. Smart Grid*, vol. 2, no. 1, pp. 131–138, Mar. 2011.

[20] E. Sortomme and M. A. El-Sharkawi, "Optimal combined bidding of vehicle-to-grid ancillary services," *IEEE Trans. Smart Grid*, vol. 3, no. 1, pp. 70–79, Mar. 2012.

[21] W. Li, X. Tan, B. Sun, and D. H. K. Tsang, "Optimal power dispatch of a centralised electric vehicle battery charging station with renewables," *IET Commun.*, vol. 12, no. 5, pp. 579–585, Mar. 2018.

[22] K. Kaur, N. Kumar, and M. Singh, "Coordinated power control of electric vehicles for grid frequency support: MILP-based hierarchical control design," *IEEE Trans. Smart Grid*, vol. 10, no. 3, pp. 3364–3373, May 2019.

[23] S. Han, D. Lee, and J.-B. Park, "Optimal bidding and operation strategies for EV aggegators by regrouping aggregated EV batteries," *IEEE Trans. Smart Grid*, vol. 11, no. 6, pp. 4928–4937, Nov. 2020.

[24] Y. Zheng, Z. Shao, X. Lei, Y. Shi, and L. Jian, "The economic analysis of electric vehicle aggregators participating in energy and regulation markets considering battery degradation," *J. Energy Storage*, vol. 45, Jan. 2022, Art. no. 103770.

[25] W. Yao, J. Zhao, F. Wen, Z. Dong, Y. Xue, Y. Xu, and K. Meng, "A multi-objective collaborative planning strategy for integrated power distribution and electric vehicle charging systems," *IEEE Trans. Power Syst.*, vol. 29, no. 4, pp. 1811–1821, Jul. 2014.

[26] O. Erdinç, A. Tascikaraoglu, N. G. Paterakis, I. Dursun, M. C. Sinim, and J. P. S. Catalão, "Comprehensive optimization model for sizing and siting of DG units, EV charging stations, and energy storage systems," *IEEE Trans. Smart Grid*, vol. 9, no. 4, pp. 3871–3882, Jul. 2018.

[27] Y. Zheng, Z. Y. Dong, Y. Xu, K. Meng, J. H. Zhao, and J. Qiu, "Electric vehicle battery charging/swap stations in distribution systems: Comparison study and optimal planning," *IEEE Trans. Power Syst.*, vol. 29, no. 1, pp. 221–229, Jan. 2014.

[28] E. C. da Silva, O. D. Melgar-Dominguez, and R. Romero, "Simultaneous distributed generation and electric vehicles hosting capacity assessment in electric distribution systems," *IEEE Access*, vol. 9, pp. 110927–110939, 2021.

[29] D. F. Recalde Melo, A. Trippe, H. B. Gooi, and T. Massier, "Robust electric vehicle aggregation for ancillary service provision considering battery aging," *IEEE Trans. Smart Grid*, vol. 9, no. 3, pp. 1728–1738, May 2018.

[30] D. Liu, L. Wang, M. Liu, H. Jia, H. Li, and W. Wang, "Optimal energy storage allocation strategy by coordinating electric vehicles participating in auxiliary service market," in *Proc. IEEE Access*, vol. 9, 2021, pp. 95597–95607.

[31] (2024). *Electric Reliability Council of Texas (ERCOT)*. Accessed: Jan. 24, 2024. [Online]. Available: http://www.ercot.com/

[32] (2024). *California Independent System Operator (CAISO)*. Accessed: Jan. 24, 2024. [Online]. Available: http://www.caiso.com/pages/default.aspx

[33] A. Muqbel, "Market-based planning of electric vehicle and battery storage system aggregators," Master's thesis, Dept. Elect. Eng., King Fahd Univ. Petroleum Minerals, Dhahran, Saudi Arabia, 2019.

[34] Y. Wang, N. Zhang, H. Li, J. Yang, and C. Kang, "Linear three-phase power flow for unbalanced active distribution networks with PV nodes," *CSEE J. Power Energy Syst.*, vol. 3, no. 3, pp. 321–324, Sep. 2017.

[35] H. Yuan, F. Li, Y. Wei, and J. Zhu, "Novel linearized power flow and linearized OPF models for active distribution networks with application in distribution LMP," *IEEE Trans. Smart Grid*, vol. 9, no. 1, pp. 438–448, Jan. 2018.

[36] K. Masteri, B. Venkatesh, and W. Freitas, "A fuzzy optimization model for distribution system asset planning with energy storage," *IEEE Trans. Power Syst.*, vol. 33, no. 5, pp. 5114–5123, Sep. 2018.

[37] M. Asensio, G. Muñoz-Delgado, and J. Contreras, "Bi-level approach to distribution network and renewable energy expansion planning considering demand response," *IEEE Trans. Power Syst.*, vol. 32, no. 6, pp. 4298–4309, Nov. 2017.

[38] J. M. Home-Ortiz, M. Pourakbari-Kasmaei, M. Lehtonen, and J. R. S. Mantovani, "A mixed integer conic model for distribution expansion planning: Matheuristic approach," *IEEE Trans. Smart Grid*, vol. 11, no. 5, pp. 3932–3943, Sep. 2020.

[39] S. B. Peterson, J. F. Whitacre, and J. Apt, "The economics of using plug-in hybrid electric vehicle battery packs for grid storage," *J. Power Sources*, vol. 195, no. 8, pp. 2377–2384, Apr. 2010.

[40] E. Sortomme and M. A. El-Sharkawi, "Optimal scheduling of vehicle-to-grid energy and ancillary services," *IEEE Trans. Smart Grid*, vol. 3, no. 1, pp. 351–359, Mar. 2012.

[41] A. Aldik, A. T. Al-Awami, E. Sortomme, A. M. Muqbel, and M. Shahidehpour, "A planning model for electric vehicle aggregators providing ancillary services," *IEEE Access*, vol. 6, pp. 70685–70697, 2018.

[42] W. H. Kersting, "Radial distribution test feeders," *IEEE Trans. Power Syst.*, vol. 6, no. 3, pp. 975–985, Feb. 1991.

[43] W. H. Kersting, "Radial distribution test feeders," in *Proc. IEEE Power Eng. Soc. Winter Meeting Conf.*, Jul. 2001, pp. 908–912.

[44] A. T. Al-Awami, N. A. Amleh, and A. M. Muqbel, "Optimal demand response bidding and pricing mechanism with fuzzy optimization: Application for a virtual power plant," *IEEE Trans. Ind. Appl.*, vol. 53, no. 5, pp. 5051–5061, Sep. 2017.

[45] M. Ansari, A. T. Al-Awami, E. Sortomme, and M. A. Abido, "Coordinated bidding of ancillary services for vehicle-to-grid using fuzzy optimization," *IEEE Trans. Smart Grid*, vol. 6, no. 1, pp. 261–270, Jan. 2015.

[46] S. Faddel, A. T. Al-Awami, and M. A. Abido, "Fuzzy optimization for the operation of electric vehicle parking lots," *Electr. Power Syst. Res.*, vol. 145, pp. 166–174, Apr. 2017.

[47] A. Muqbel, A. T. Al-Awami, and M. Parvania, "Optimal planning of distributed battery energy storage systems in unbalanced distribution networks," *IEEE Syst. J.*, vol. 16, no. 1, pp. 1194–1205, Mar. 2022.

AMMAR M. MUQBEL (Student Member, IEEE) received the B.Sc. and M.Sc. degrees in electrical engineering from the King Fahd University of Petroleum and Minerals, Dhahran, Saudi Arabia, in 2016 and 2018, respectively. He is currently a Lecturer with the King Fahd University of Petroleum and Minerals. His current research interest includes the operation and planning of smart grids.

ALI T. AL-AWAMI (Senior Member, IEEE) received the B.Sc. and M.Sc. degrees in electrical engineering from the King Fahd University of Petroleum and Minerals (KFUPM), Dhahran, Saudi Arabia, in 2000 and 2005, respectively, and the Ph.D. degree in electrical engineering from the University of Washington, Seattle, WA, USA, in 2010. His industrial experiences include working with Saudi Electricity Company, Saudi Arabia, and Bonneville Power Administration, USA. He is currently an Associate Professor with the Department of Electrical Engineering, KFUPM. His research interests include power system operation and optimization, and the integration of distributed energy resources into smart grids. He received several best conference papers and best student poster awards from a number of conferences, including the IEEE Power and Energy Society General Meeting, in 2009, the IEEE Clemson University Power Systems Conference, in 2016, and the Saudi Smart Grid Conferences, in 2013 and 2018.

ADNAN S. AL-BUKHAYTAN (Student Member, IEEE) received the B.Sc. degree in electrical engineering from King Faisal University (KFU), Al-Ahsa, Saudi Arabia, in 2018, and the M.Sc. degree in electrical engineering from the King Fahd University of Petroleum and Minerals (KFUPM), Dhahran, Saudi Arabia, in 2021, where he is currently pursuing the Ph.D. degree. His research interests include power system operation and optimization, and integrating distributed energy resources into smart grids.